ISPRS Open Journal of Photogrammetry and Remote Sensing 8 (2023) 100036

Contents lists available at ScienceDirect

ISPRS Open Journal of Photogrammetry and Remote Sensing

journal homepage: www.journals.elsevier.com/isprs-open-journal-of-photogrammetry-and-remote-sensing

Spatial patterns of biomass change across Finland in 2009–2015

Markus Haakana *, Sakari Tuominen, Juha Heikkinen, Mikko Peltoniemi, Aleksi Lehtonen

Natural Resources Institute Finland (Luke), Latokartanonkaari 9, FI-00790, Helsinki, Finland

ARTICLE INFO

Keywords:
National forest inventory (NFI)
Multi-source national forest inventory (MS-NFI)
Biomass change
Greenhouse gas emissions

ABSTRACT

Forest characteristics vary largely at the regional level and in smaller geographic areas in Finland. The amount of greenhouse gas emissions is related to changes in biomass and the soil type (e.g. upland soils vs. peatlands). In this paper, estimating and explaining spatial patterns of tree biomass change across Finland was the main interest. We analysed biomass changes on different soil and site types between the years 2009 and 2015 using the Finnish multi-source national forest inventory (MS-NFI) raster layers. MS-NFI method is based on combining information from satellite imagery, digital maps and national forest inventory (NFI) field data. Automatic segmentation was used to create silvicultural management and treatment units. An average biomass estimate of the segmented MS-NFI (MS–NFI–seg) map was 73.9 tons ha^{-1} compared to the national forest inventory estimate of 76.5 tons ha^{-1} in 2015. Forest soil type had a similar effect on average biomass in MS–NFI–seg and NFI data. Despite good regional and country-level results, segmentation narrowed the biomass distributions. Hence, biomass changes on segments can be considered only approximate values; also, those small differences in average biomass may accumulate when map layers from more than one time point are compared. A kappa of 0.44 was achieved for precision when comparing undisturbed and disturbed forest stands in the segmented Global Forest Change data (GFC-seg) and MS–NFI–seg map. Compared to NFI, 69% and 62% of disturbed areas were detected by GFC-seg and MS–NFI–seg, respectively. Spatially accurate map data of biomass changes on forest land improve the ability to suggest optimal management alternatives for any patch of land, e.g. in terms of climate change mitigation.

1. Introduction

In the European Union (EU), forest land is an important category in the Land Use, Land-Use Change and Forestry (LULUCF) sector, absorbing nearly 9% of total emissions of other sectors in 2019 (European Environment Agency, 2021). However, forest characteristics vary largely at the regional level and in smaller geographic areas. The amount of greenhouse gas emissions is related to changes in biomass and for example to the soil type (e.g. mineral soils vs. peatlands). Peatlands have huge potential in climate change mitigation (Leifeld and Menichetti, 2018). Peatland forests cover nearly 8% of forest land in the EU; the proportion is highest in the boreal zone. In Finland peatlands cover 27% of forest land, and most of it (72%) is drained. Consequently, largest emissions within forest land result from drained peatlands in Finland (Statistics Finland, 2021). Forest characteristics affect the forest management practices and how vulnerable single stands are to disturbances. Biomass losses, disturbances and decomposition result in greenhouse gas emissions (Herold et al., 2019). Hence, spatially accurate maps are valuable for forest resource management (Herold et al., 2019), and for precision forest management where decisions are made based on accurately determining forest characteristics (Holopainen et al., 2014).

Various types of remote sensing data have been used for monitoring forest biomass. Typically, optical satellite imagery, field measurements and allometric models on the basis of field measurements are used in remote sensing-based mapping and monitoring of biomass (Tuominen et al., 2010; Hirata et al., 2014; Saarela et al., 2020; Li et al., 2020). Use of satellite data allows very large area biomass mapping, even continental level (Kindermann et al., 2008; Gallaun et al., 2010). More accurate map predictions of biomass (especially for small areas) can be achieved by using airborne laser scanning (ALS) which is considered the most accurate remote sensing data in estimating growing stock and biomass variables, due to the 3-dimensional canopy modelling capability of the data (Tuominen and Haapanen, 2013; Saarela et al., 2020). The drawback of ALS is the high cost of the data, which limits the area coverage and temporal resolution of the data. Active satellite sensors such as satellite-based radar have been used for biomass mapping, but in

* Corresponding author.
E-mail address: markus.haakana@luke.fi (M. Haakana).

https://doi.org/10.1016/j.ophoto.2023.100036
Received 14 April 2022; Received in revised form 22 March 2023; Accepted 11 April 2023
Available online 11 April 2023

general, their main advantage over optical satellite sensors in biomass mapping is their capability the penetrate cloud cover (Tokola et al., 2007; Holopainen et al., 2014; Lohberger et al., 2011). Satellite based Global Ecosystem Dynamics Investigation (GEDI) allows large area coverage combined with 3D data for biomass mapping (Saarela et al., 2018), but the main drawback of the sensor is the low spatial resolution of mapping and limited latitudinal range of the instrument.

During the last two decades, several maps of biomass and forest cover have been produced at global and regional scales, in many cases at coarse resolution, e.g. Hansen et al. (2003) and Kindermann et al. (2008). At a regional level, higher resolution biomass maps are also available, but in some cases, they have limitations in the available *in situ* data or the sensitivity of satellite sensors to forest biomass (Rodríguez-Veiga et al., 2016). Global Forest Change layers (Hansen et al., 2003) have been used with biomass maps to quantify biomass loss due to harvests on forest land. However, results at the European and country level show that biomass densities vary regionally, causing decreasing correlation between harvested areas and actual biomass loss. According to Ceccherini et al. (2020), biomass loss has increased by 69% between the periods of 2011–2015 and 2016–2018. This finding has been challenged and found to be conflicting with national statistics (Picard et al., 2021).

Direct field-based NFI measurements produce accurate reference data (Egusa et al., 2020), which can be used for the validation of biomass maps. Several countries have NFI data available, especially in the EU. However, it is often not regularly measured or up-to-date hindering biomass map validation (Avitabile and Camia, 2018). In Finland, NFI data are continuously measured at a five-year inventory cycle. Besides, the Finnish Multi-Source National Forest Inventory (MS-NFI) provides multi-temporal thematic raster layers for the whole country on large number of forest variables at a pixel resolution of 16 m, e.g. timber volume and biomass by tree species, land-use class and site type. MS-NFI data is based on satellite images (Landsat 5 TM/7 ETM+/8 OLI, Sentinel 2A-MSI, IRS P6, ALOS AVNIR-2), digital maps and NFI field data and is produced every second year (Tomppo and Halme, 2004; Tomppo et al., 2008a; Mäkisara et al., 2019). In many other countries, similar products are provided (Reese et al., 2003; Gjertsen, 2007; Barrett et al., 2016; Nilsson et al., 2017; Katila and Heikkinen, 2020). Where NFI data are not available, ALS have been successfully used for validating and calibrating satellite based estimates with larger spatial coverage. Combining ALS and Landsat satellite time series have also been used with random forest model (R package) to estimate forest structure across different site types (Bolton et al., 2020). Biomass density maps based on remotely sensed data can be used to enhance field inventory stratification to provide estimates on under-sampled or unapproachable areas (ISPRA, 2021; Vangi et al., 2023).

High resolution and high accuracy estimate on tree biomass and its changes are essential to policy makers and to forest owners for targeting climate change mitigation and adaptation actions (Herold et al., 2019). Currently, climate change mitigation initiatives have connections to the forest owner level, when governments support forest management practices, that increase carbon sequestration or reduce GHG emissions from forests. In addition, the forest industry is interested in compensating for their CO_2 emissions, where forest management actions could provide feasible ways to increase carbon sinks. Also, soil carbon modelling community benefit from accurate biomass maps, as those can be used to derive litter fall estimates that are needed for soil C simulations.

Stands are the basic units for forest management and forestry practices prefer relatively permanent stand boundaries. Formerly, stand boundaries were delineated manually based on the interpretation of aerial photographs. Currently, they are mainly delineated automatically based on digital remote sensing data. Stands delineated from raster format thematic map data of MS-NFI based on automatic image segmentation can be used as the units for modelling of carbon cycles in forests. Pixel-based classification often has a large variation with neighbouring pixels (Yu et al., 2006; Kim et al., 2011). In our study, we created homogeneous units by segmentation, which could be further applied in targeted climate change mitigation studies. In Finland, it is essential to delineate peatland from mineral soils due to remarkably different forest management treatments and accessibility (Pukkala, 2020), and in addition, the drainage situation of peatland soils strongly affects GHG emissions. Site fertility is related to growth rate and soil GHG exchange estimation, and it is therefore important in segmentation, as well as growing stock characteristics (Mustonen et al., 2008).

Our motivation for this study was to compute a segmented biomass map according to soil type, volumes of growing stock per main tree species and property borders to facilitate spatial GHG exchange estimation. Biomass densities and their changes were estimated for the segments. In this study, we utilized MS-NFI data from 2009 to 2015 to derive above and below ground biomass for the segments and investigate spatio-temporal variation of biomass. With stand level soil carbon modelling, it is essential to know the amount of biomass in forest stands and which kind of forests management actions have been done, e.g. allocation of felling sites, when seeking best solutions in forest management to mitigate climate change. Reference data for overall above ground and below ground biomass estimates were derived from NFI. In our study, estimating tree biomass change and explaining spatial patterns across Finland were the main interests. For this we analysed biomass changes on different soil types on forested land. The specific objectives of the study were (1) to produce segmented fine resolution maps on tree biomass and its changes, (2) to evaluate accuracy and usefulness of segmented biomass maps and biomass change maps, (3) to retrieve stand-replacement harvest map based on biomass changes and evaluate its precision with corresponding Global Forest Change data by Hansen et al. (2013).

2. Materials

2.1. Study area

The study area covers whole Finland ranging from hemiboreal to subarctic zone (59°40′- 70°05′ N; 19°05′ - 31°35′ E) (Fig. 1). The main tree species are Scots pine (*Pinus sylvestris*), Norway spruce (*Picea abies*), and birch species (*Betula* spp.) as well as other deciduous species (mostly *Populus tremula* and *Alnus* spp.). The forested area covers approximately 70% of the land area and is nearly entirely in the boreal zone. Topography varies typically from sea level to 200 m a.s.l., in Southern Finland, while higher hills are located in Northern Finland, where there is also a transition from forest zone to alpine tundra on the fell tops. The treeline in the north varies between 200 and 450 m a.s.l. (Franke et al., 2019).

Forestry is active everywhere and on all types of forest lands where it is considered economically profitable. Exceptions are northernmost Finland and conservation areas. Forests in southern Finland consist mainly of productive land with small rocky hills or mires. Forests are less productive in the North and the proportion of peatland forests is larger. Protected areas are 8.2% on forest land or 12.6% with poorly productive forest land (strictly protected forests, class 1; and protected forests on biodiversity conversation sites where cautious fellings are allowed, class 2) (Luonnonvarakeskus, 2022). Most of the protected areas are in Northern Finland.

2.2. Field data

National forest inventory (NFI) field data were used as a reference data in the study. NFI field plot data are based on systematic cluster sampling (Korhonen et al., 2017). We used data from the tenth NFI (NFI10 2004-2008), eleventh NFI (NFI11 2009-2013) and available data from the twelfth NFI (NFI12 2014-2017). The total number of sample plots in NFI varies between inventory cycles but is between 60 000 and 70 000 plots on land areas. NFI data are also used in the Finnish greenhouse gas inventory in biomass estimation (Statistics Finland,

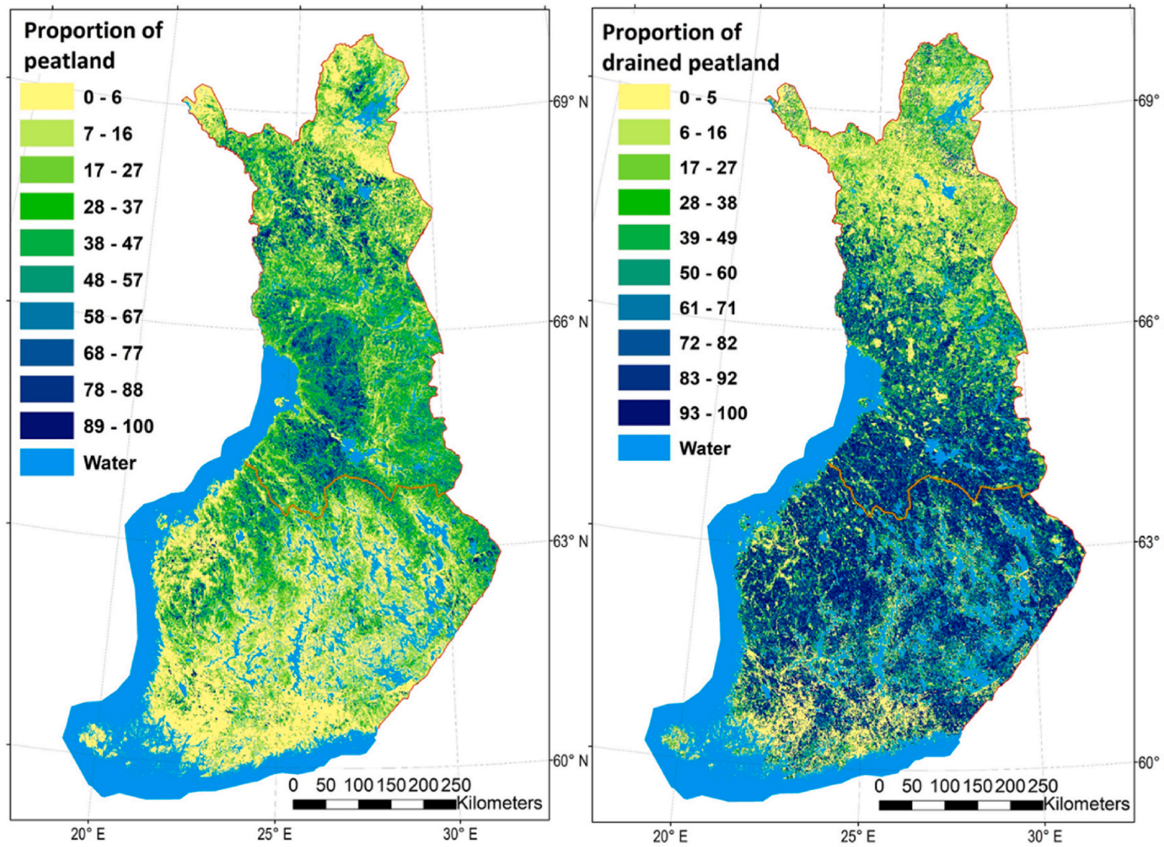

Fig. 1. Proportion of peatlands of total forestry land (left) and proportion of drained peatlands of the total area of forestry land on peatlands (right) calculated in 1-km^2 raster pixels. A borderline of southern and northern Finland (orange line on panels) shows the division is applied with greenhouse gas inventory data, which was also used in the Results section. (For interpretation of the references to colour in this figure legend, the reader is referred to the Web version of this article.)

2021). Trees in NFI are measured whether they are sample trees or tally trees. Sample trees have larger numbers of measured parameters, and on tally trees, only basic parameters are recorded and measured, e.g. tree species and diameter at breast height (1.3 m). Biomass estimates are first predicted for sample trees by the wood density and biomass models (Repola et al., 2007; Repola, 2008, 2009). Biomass estimates of tally trees are based on estimates of sample trees and the parameters of tally trees and stands (Korhonen et al., 2013, 2017; 2021). Accomplished management measures, such as cutting types and years are recorded for the sample plots. In the NFI, the national definition of forest land is based on annual average growth including bark (at least 1 m^3 ha^{-1} a^{-1}); sites with growth in 0.1–1 m^3 ha^{-1} a^{-1} are classified as poorly productive forest land. Forested land is the combination of these two classes. In this study, we also consider the FAO/FRA definition of forest land, which is applied in Finnish greenhouse gas inventory. The FAO/FRA forest land is defined as land with trees higher than 5 m and a canopy cover of more than 10% or trees able to reach these thresholds *in situ* (Statistics Finland, 2021). FAO/FRA forest land includes all nationally defined forest land, the most fertile part of poorly productive forest land and other areas such as forestry roads and depots.

2.3. Multi-source national forest inventory (MS-NFI) data

Multi-source national forest inventory (MS-NFI) of Finland produces thematic map layers of forest variables such as volume of growing stock and biomass (Tomppo, 1991, 2006; Tomppo et al., 2008a; Mäkisara et al., 2016). MS-NFI data has approx. 2–3 years interval between consecutive update of the map layers. MS-NFI is used for combining information from field measurements of national forest inventory (NFI) plots, remote sensing imagery (such as Landsat or Sentinel) and digital maps. Optical satellite imagery pixel values are used for predicting the forest variables of (non-measured) satellite image pixels by non-parametric k nearest neighbour (k-NN) method. In the k-NN method k spectrally most similar NFI plots (i.e., nearest in the satellite image spectral feature space) are defined for each satellite image pixel, and the predicted values of forest variables are calculated as weighted averages of the nearest neighbours (i.e. NFI plots). Digital maps are used for separating forestry land from other land use to which forest variables are not predicted. Also, digital maps are used for stratification of forestry land between mineral lands and peatlands, which generally tends to improve the accuracy of predicted data, since the peatland and mineral land forests have slightly differing characteristics (as regards of the growing stock).

MS-NFI thematic maps include over 40 themes on forest parameters such as growing stock volume by tree species (m^3 ha^{-1}), site fertility class, biomass by tree species (there are four species groups) in subclasses, e.g. biomass of spruce foliage (10 kg ha^{-1}). In this study, we used MS-NFI biomass layers from 2009 to 2015. The MS–NFI–2009 thematic maps were based on tenth and eleventh NFI sample plot data measured in 2006–2008 and 2009–2010, respectively. The satellite imagery consisted of 38 Landsat 5 TM scenes, which were complemented with 14 Landsat 7 TM scenes, 3 IRS P6 LISS III scenes and 10 ALOS AVNIR-2 scenes (Tomppo et al., 2013). The images were acquired between May 29th and August 22nd' 2009, additionally 5 image scenes were acquired in 2010 between dates June 1st and August 17th. The image acquisition date range indicates that it may be quite difficult to achieve a full cloud free satellite image coverage from the leaf-on season of one year, as would be required by MS-NFI. The full list of utilized images is presented in Tomppo et al. (2013). The digital map data originates from the National Land Survey of Finland (NLS) and was rasterised with a 20-m pixel size in the MS-NFI (Tomppo et al., 2013).

In the MS–NFI–2015, the field data originated from eleventh and twelfth NFI inventory from measurement years 2012–2013 and 2014–2016, respectively. The NFI tree data were updated computationally by growth models to the date 31 July 2015. This time the employed satellite imagery consisted of 43 Landsat 8 OLI scenes and 1 Sentinel-2A MSI scene. Satellite images were acquired between July 3rd and September 10th, 2015. Additionally, one scene was from August 18th' 2016 (Mäkisara et al., 2019). Although the improved spatial and spectral resolution of Sentinel 2 imagery offer an advantage over Landsat imagery, the operational availability of the Sentinel 2 imagery was still very limited. In the MS–NFI–2015 data product, satellite images and other datasets were resampled to 16 m resolution. Some areas covered by clouds were completed by the previous MS-NFI products (in MS–NFI–2015, approximately 1.2% of forestry area), in compilation sub-products from years 2000–2015 (Mäkisara et al., 2019). In MS-NFI, numerical maps of NLS were used to exclude other land classes from forestry land (e.g. arable land, roads and other built-up lands, Tomppo et al., 2013; Mäkisara et al., 2019). The MS-NFI maps are open access data, available at: https://kartta.luke.fi/index-en.html.

3. Methods

3.1. Automatic segmentation of MS-NFI layers

Grid cell data was aggregated to larger continuous areas to resemble forest management units, which were applied in the allocation of felling sites with forest cover loss and estimation of tree biomass and its change within units. Image segmentation was used for delineating forest stands from MS-NFI thematic maps. Image segmentation is a technique that aims at producing spatially continuous and disjointed units that are sufficiently homogeneous in relation to desired characteristics (Haralick and Shapiro, 1985). There are several alternative strategies for the segmentation of raster data, such as edge detection, region extraction, feature thresholding or clustering (Fu and Mui, 1981). The edge detection-based methods aim at recognizing edges, i.e. locations of significant changes in input data, such as stand borders. The process is local and thus, it does not assume spectral uniformity over the segmented area. In addition, segmentation requires linking the detected edges into relevant boundaries for composing appropriate spatial inventory units (i.e. stands). In the automatic segmentation we aimed at spatially continuous areas that are homogeneous by their stand and soil properties. For this purpose we utilized segmentation algorithm that combines features of edge- and region-based approaches: "Image segmentation with directed trees" (Narendra and Goldberg, 1980). We applied software that utilizes a slightly modified implementation of the algorithm by Pekkarinen (2002, 2004).

The segmentation method employs the local edge gradient for recognizing potential segment borders. Segmentation covered forest land, poorly productive forest land and unproductive land, from which subsets of segments were selected for the study. Volumes of growing stock per main tree species (m^3 ha^{-1}) estimated in MS–NFI–2015, soil type (mineral soils, drained organic and undrained organic soils) and property borders derived from National Land Survey vector data were used as segmentation criteria. The drainage situation was computed based on NLS topographic database, where drainage was defined using a 40-m buffer around artificial ditches. We produced segmented biomass maps and biomass change maps from MS-NFI layers as segment averages for the whole country. The class variables, like soil type and site fertility type used in the evaluation, were treated as mode variables in the segmentation. The same segment boundaries were applied for MS–NFI–2009 data.

3.2. Validation of biomass maps

The data from NFI were used to evaluate biomass maps. We analysed biomass stocks and distribution in NFI, MS-NFI and MS-NFI segmented data (MS–NFI–seg). The NFI results on biomass stocks based on measurement years 2013–2017 were aggregated separately for southern and northern Finland from regional statistics (Luonnonvarakeskus, 2019), where NFI data comprised the forested land area. Corresponding results for MS-NFI and MS–NFI–seg layers were derived from layer histograms. Only one year NFI data, corresponding MS-NFI time points (2009 or 2015), were used for the biomass distribution analyses to avoid changes in biomass due to timber harvests or any land-use changes. MS-NFI map features were extracted to the NFI plots for the analyses. Additionally, to compare the regionally summed segmented biomass stocks to the ones reported in the Finnish GHG inventory, we applied the FAO/FRA forest land definition. The GHG biomass stocks were calculated separately for mineral soils, undrained and drained peatland forests on FAO/FRA forest land (Statistics Finland, 2021). Uncertainty associated with the NFI estimates of biomass stock was estimated as standard error due to sampling (see Tomppo et al., 2011, sec. 3.5., for details). Uncertainty due to estimation of biomass model parameters was not included, because it has no impact on validation: Both NFI and MS-NFI utilise the same models with the same errors in parameters.

Table 1 shows forest areas in NFI, GHG and MS-NFI data. NFI forested land is slightly smaller than the corresponding area in the MS–NFI–2015 layer. NFI classification is based on both land use and land cover. Therefore, in NFI, other land uses include lands with tree cover, e.g. small forest strips on built-up land. MS-NFI forest masks are based on NLS digital maps. Satellite image mosaics of MS–NFI–2009 and MS–NFI–2015 are presented by Tomppo et al. (2013) and Mäkisara et al. (2019). Biomass changes were calculated for areas, where both MS–NFI–2009 and MS–NFI–2015 had cloud-free cover. A large part of northernmost Finland was covered by clouds; however, due to climate and altitude, only minor part of that area fulfils forest land definition. Otherwise, the remaining cloudy areas were mostly in western and northern Finland as shown in Fig. 2. Average change in biomass comparisons were derived directly from cloud-free images. The change layer between MS–NFI–2009-seg and MS–NFI–2015-seg includes cloud-free areas. To evaluate the effect of biomass model errors on results, we compared also basal areas estimates between NFI, MS-NFI and MS–NFI–seg data. These results are provided in the Supplementary material.

3.3. Forest cover change in time-series

3.3.1. General

We selected the length of study period so that areas with biomass gains due to growth could potentially be separated from those of biomass losses due to harvests and other disturbances. The mean biomass gross increment on forest land were 3.4 t ha^{-1} a^{-1} or 20.0 t ha^{-1} within the whole study period (Statistics Finland, 2021). Ideally, losses are detected in each stand when stands are harvested or affected by disturbances. It has been reported, for example, that MS-NFI stem volume predictions are saturated for stands over 200 m^3 ha^{-1} (Vastaranta et al., 2014). Therefore, false losses in tree biomass derived from MS-NFI products may occur for stands with large biomass or volume. Detecting biomass gains, on the other hand, may require aggregation of several stands, in time-series analyses significant trends have been found with a

Table 1
Forest-related areas in different datasets and total area of Finland including inland waters.

Dataset and area attribute	Total, 1000 ha
MS–NFI–2015, Total area	33 830
MS–NFI–2015, Forested land	23 494
NFI, Forested land	21 943
GHG-2009, Forest land	21 882
GHG-2015, Forest land	21 371
MS–NFI–seg change, Forested land (cloud free)	22 813

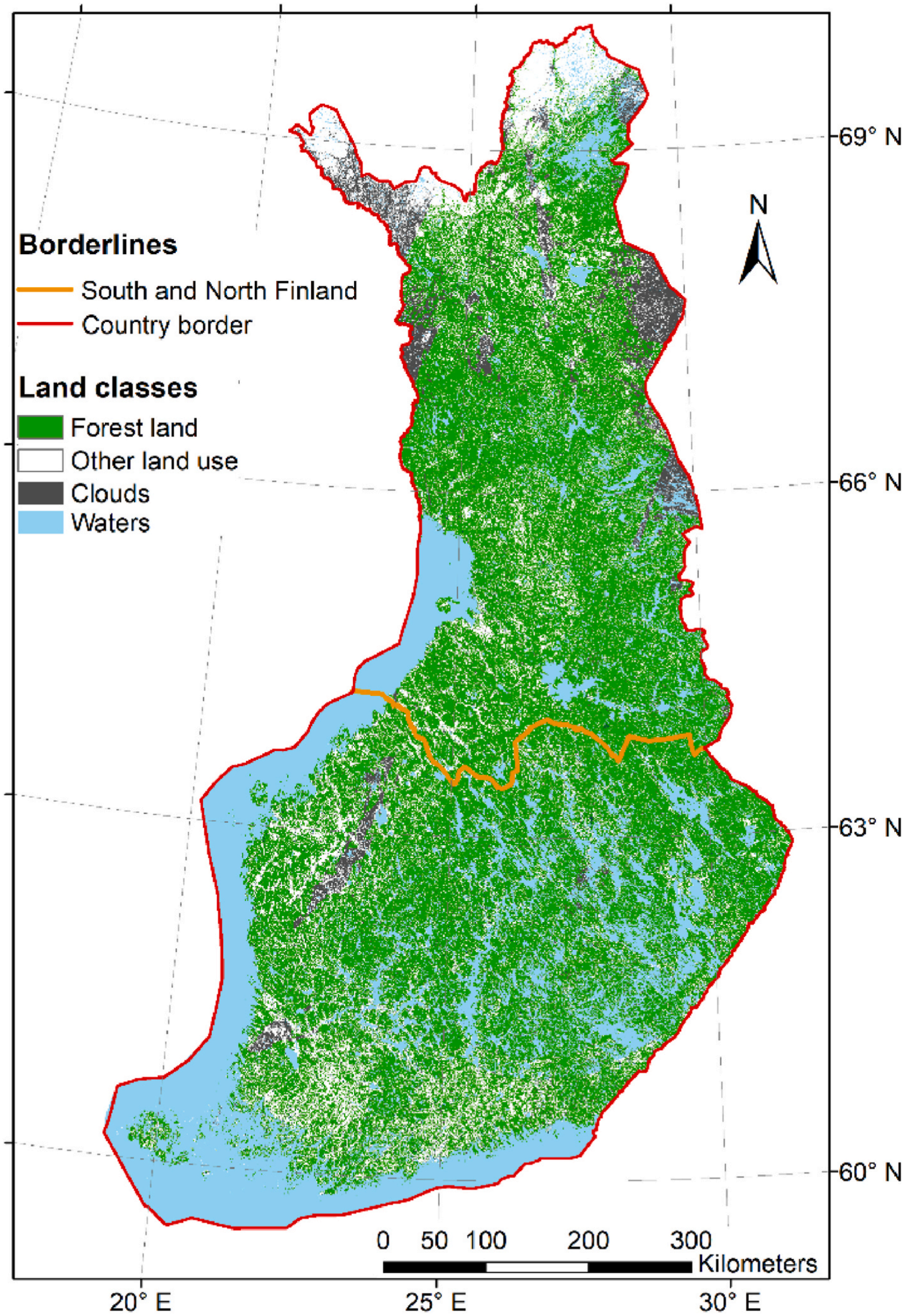

Fig. 2. FAO Forest land (green), other land use (white), waters (blue). Clouded areas (grey) on forest land, i.e. no estimate. (For interpretation of the references to colour in this figure legend, the reader is referred to the Web version of this article.)

relatively large unit size, 1200 × 1200 m^2 (Katila et al., 2020). In NFI11, mean volumes on mature stands on forest land were 251 m^3 ha^{-1} and 134 m^3 ha^{-1} in southern and northern Finland, respectively.

3.3.2. *Biomass gains*

As stated in general section of this chapter, annual gains are relatively small and therefore a study period of several years was selected to better separate areas with biomass gains from those with biomass losses. Gains are detected when biomass is greater in MS–NFI–2015-seg layer than in MS–NFI–2009-seg layer.

3.3.3. *Biomass losses*

To detect areas with stand-replacement harvests or disturbances, a threshold of 50% of mean biomass loss was used for the MS–NFI–seg data. We compared our forest cover loss estimates to those estimated in the Global Forest Change (GFC) dataset (Hansen et al., 2013) to evaluate the precision of that product and the conclusion given by Ceccherini et al. (2020). GFC data shows stand replacement in cases where stand height has decreased below the threshold for forest land, i.e. 5 m of height. We downloaded the 2018 forest cover losses layer and applied yearly estimates from years between 2009 and 2015, version Hansen_GFC-2018-v1.6_lossyear_40N_080W.tif. Hansen's GFC loss map was resampled on the same grid as the MS-NFI data at 16-m resolution using a nearest-neighbour method. A segment was considered as disturbed if more than 40% of the area had forest cover loss in GFC segmented dataset (GFC-seg). To compare segment level observations to NFI field data on regeneration cuttings, we selected plots measured in 2015. If regeneration cuttings were accomplished in the measurement year or five years prior to that, then the plot was considered as disturbed.

4. Results

4.1. Biomass estimates and distributions

MS–NFI–seg and MS-NFI total biomass estimates were close to NFI values and means of biomass were slightly lower than those that were calculated from NFI plots (Table 2). Average basal areas according to protection status of forests are presented in the Supplementary material (Fig. S1).

NFI field data shows the greatest variation with a larger number of plots on data extremes on both inventory rounds (Fig. 3). However, MS–NFI–2009 data had very similar frequency and biomass values to NFI11 (NFI measured in 2009–2013). MS–NFI–2015 preserved also largely the distribution pattern as in NFI12 (NFI measurement years 2014–2017 included) except for the lower end. Segmentation showed higher average biomass values at the lower end of the frequency distribution and on the other hand, the highest values were lower than in NFI. Corresponding patterns are shown also for basal areas in the Supplementary material (Fig. S2 and Fig. S3). The density plot on 2009 and 2015 data shows that NFI has a relatively large number of plots with very low biomass, and plots with biomass values of more than 200 tons per hectare. Distributions MS-NFI and MS–NFI–seg data show that the largest and lowest values are averaged in the estimation process, which is the expected result (Fig. 3). The proportion of plots with over 200 tons per hectare biomasses were 5.0% and 0.1% in NFI11 and MS–NFI–2009-seg data, respectively. The corresponding proportions in NFI12 and MS–NFI–2015-seg data were 6.1% and 0.8%, respectively.

Correlation diagrams of MS–NFI–2015 and MS–NFI–2015-seg data showed similar patterns of biomass stocks with NFI plot estimates (Fig. 4). In both cases correlation coefficients were of similar magnitude, but the slope of the fitted linear function was decreased in segmentation.

4.2. Biomass changes

Both NFI and MS–NFI–seg data showed an increase in living biomass between 2009 and 2015 (Fig. 5). In 2009, NFI resulted in slightly higher biomass values than MS–NFI–2009-seg but the average biomass values between the two datasets were still close to each other. At the same time, MS–NFI–seg showed a larger increase in biomass than NFI, i.e. 7.1 tons ha^{-1} (+10.2%) and 4.6 tons ha^{-1} (+6.1%), respectively. On mineral soils, the average biomass values were quite close to each other in NFI and MS–NFI–seg data (Fig. 6). On peatland soils, the MS–NFI–seg data showed slightly lower biomass values. Both data resulted in biomass increase between 2009 and 2015. However, relative changes in per hectare biomass were quite different in NFI and MS–NFI–seg in most cases except on mineral soils in Northern Finland. An exceptionally large difference between datasets was detected on undrained organic soils in Southern Finland, where NFI data resulted in a remarkably high increase in biomass compared to MS–NFI–seg data.

4.3. Recognition of harvested stands

Biomass change maps showed either gains or losses for each segment and a change from forest to the non-forest stage in the case of the Global Forest Change map (Fig. 7). Forested land was covered by areas of relatively small changes in biomass, according to Luke's forest statistics, approximately 3.9% of the forested land area was managed with stand-replacement harvests during the study period (Luonnonvarakeskus, 2022). It is approximately 150,000 ha a^{-1} on average. At the segment level, the corresponding proportion was 4.9% with MS–NFI–seg data and 5.2% with the GFC-seg map. In the latter case, original data without segmentation resulted in a proportion of 4.2% of forest area converted to the non-forest stage. Examples in Fig. 7 show that for most segments, biomass changes based on MS–NFI–seg maps were relatively small, and therefore, depending on the satellite image and field data in classification, it can be difficult to distinguish between small biomass growth and decrease. This was the case especially in mature stands with high biomass levels. Only segments where biomass had decreased more than a threshold of 50% were interpreted as disturbed in the MS–NFI–seg data, i.e., presented with black colour in Fig. 7. The confusion matrix examining the disturbed and undisturbed segments between MS–NFI–seg and the GFC-seg map showed 95% of correctly classified segments (Table 3). However, as the proportion of disturbed segments was very small on both data sets, the kappa value representing the success of classification was 0.44, indicating a relatively weak level of agreement between the two data sets. The producer's accuracy of the disturbed areas was 0.40, and it was 0.98 for undisturbed areas. The user's accuracies for the same classes were, respectively, 0.56 and 0.97. There were 286 disturbed plots in NFI data, GFC-seg data detected 69% of those as disturbed and MS–NFI–seg data 62%, respectively (Table 4). In addition, large number of plots was labelled as disturbed in GFC-seg and MS–NFI–seg data while in the NFI being undisturbed.

Table 2
Biomass estimates for NFI plots, MS-NFI and MS–NFI–seg.

	NFI plots 2013–2017	MS–NFI–2015	MS–NFI–2015-seg
Area, 1 000 ha	22 813	23 494	23 494
Total biomass of living trees, mill. tons	1 745	1 752	1 737
Biomass of living trees, mill. tons ha^{-1}	76.5	74.6	73.9

5. Discussion

The precision of biomass estimates on MS–NFI–seg data was explored in this study. This included biomass estimates at regional and whole country level, biomass change estimates and detection of harvested areas. The segmentation results were also tested with NFI field data at plot level. Especially for soil carbon modelling purposes achieving reliable estimates on segmentation is essential. Soil carbon modelling utilizes information from image segments on tree biomass and their changes. Compared to pixel-level MS-NFI thematic maps, MS–NFI–seg data provide an effective way for modelling by speeding up the procedures. Stand properties, such as tree species volumes, were used in delineating the segments from each other. Additionally soil characteristics and property boundaries were used in running the segmentation in this study. Therefore, image segments were not homogeneous units by stand features but were affected also by management situations. In the end, stand properties did not necessarily follow segment borders, causing mixed segments.

The assessment of the MS–NFI–seg dataset on tree biomass at the whole country level showed that the estimates were very close to those derived from MS-NFI thematic maps. Compared to NFI field data MS-NFI tend to overestimate forestry land area due to it being based on digital map masks, which are more land cover rather than land use. MS–NFI–2015 training data is different from NFI field data due to it being computationally updated to the target date, 31.7.2015, for which growth models were used, cuttings updated and parts of plots removed due to changes. The updating was performed separately for each processing window and calibrated with field data mean volumes (Mäkisara et al., 2019). Therefore, only minor differences between updated training data used in MS-NFI and original NFI field data were expected on biomass. In all, image segmentation did not introduce significant bias in mean and total biomass estimates compared to MS-NFI in Finland.

Segments are usually smaller than typical forest management and treatment units and preserve much of the original image variation. In MS-NFI, thematic maps are based on k-NN estimation, where the value of *k* varies from 3 to 5 depending on image conditions (Mäkisara et al.,

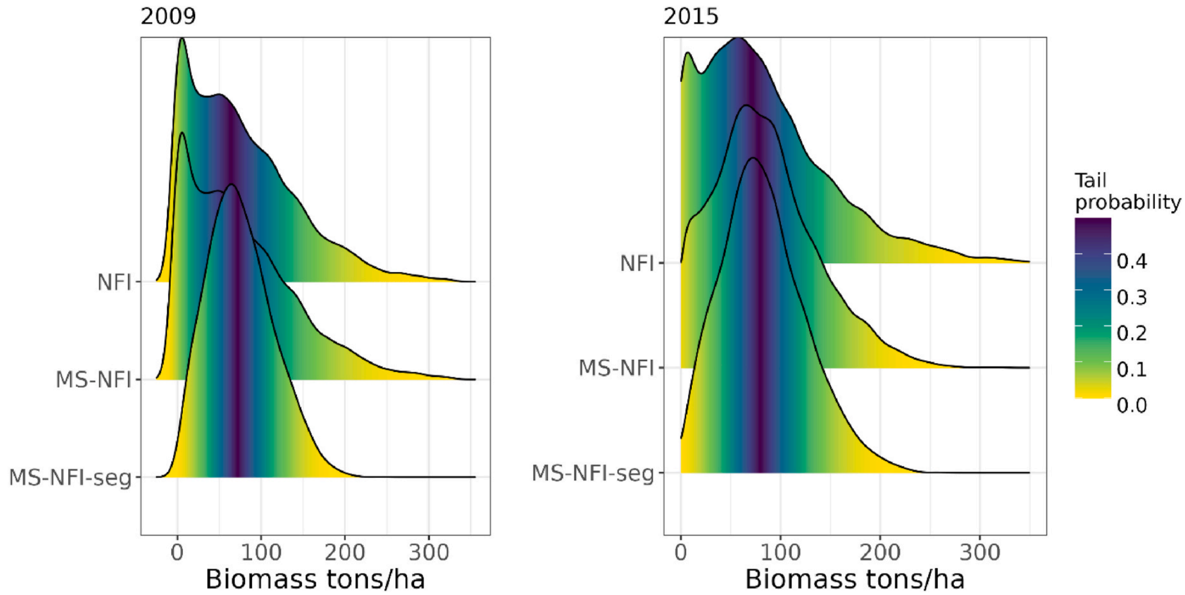

Fig. 3. Density estimates of biomass for NFI, MS-NFI and MS–NFI–seg on forested land in 2009 (n = 7590 and 2015 (n = 6853) data.

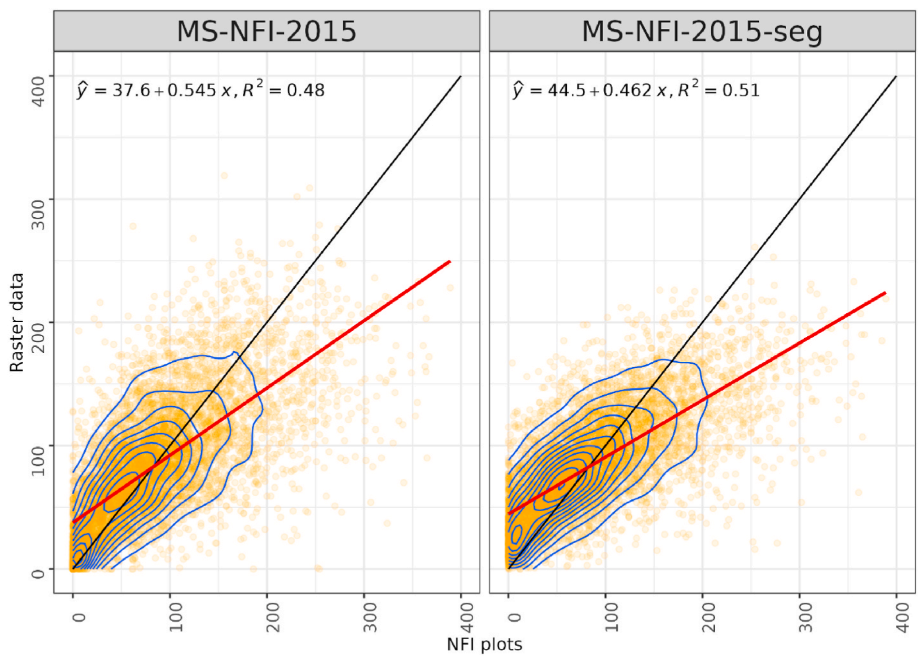

Fig. 4. Correlation of biomass stocks (tons/ha) between NFI and pixel-level MS-NFI (left) and MS–NFI–seg (right) data in 2015.

2019). When a similar variation than in field data is desired, then k = 1 is appropriate, and when RMSE minimisation is desired, then a higher value of k is presumed (Franco-Lopez et al., 2001; McRoberts et al., 2002; Katila and Tomppo, 2001). K-NN-based satellite image estimates have typically high RMSEs at the individual pixel level (Tomppo et al., 2008b), which causes undesired noise in classification results when aiming at further analyses of stand variables (Hall et al., 2006). When comparing to field data, observations on data extremes tend to be underestimated when a higher number of sample records are used, which is reported in several papers, e.g. Hall et al. (2006), Tuominen et al. (2017). Even though the highest and lowest biomass values were underestimated in segmentation maps, the country-level results corresponded well with NFI. Zheng et al. (2004) reported similar observations at regional the level. Avitabile and Camia (2018) assessed European biomass maps using harmonized statistics and field plots and reported negative bias of biomass estimates, overestimation at low biomass and underestimation at high biomass. In this study the bias remained low. The saturation of Landsat imagery is an important factor for inaccurate aboveground biomass estimation (Zhao et al., 2016). In this study, saturation was observed on protected areas and forested land available for wood production. Protected areas included areas with relatively high biomass, even though they are commonly established in areas with less than average productivity (Häkkilä et al., 2017). Approximately 12% of forested land is protected in Finland and according to the NFI mature forests cover 12% of the total forest land area. Classification results on forested land at the mature stage are predominantly affected by pixel value saturation. However, it was noted that MS–NFI–seg biomass estimates are sufficiently accurate for soil carbon modelling purposes, e.g. as an input data for a model when selecting areas where regeneration cuttings have been carried out.

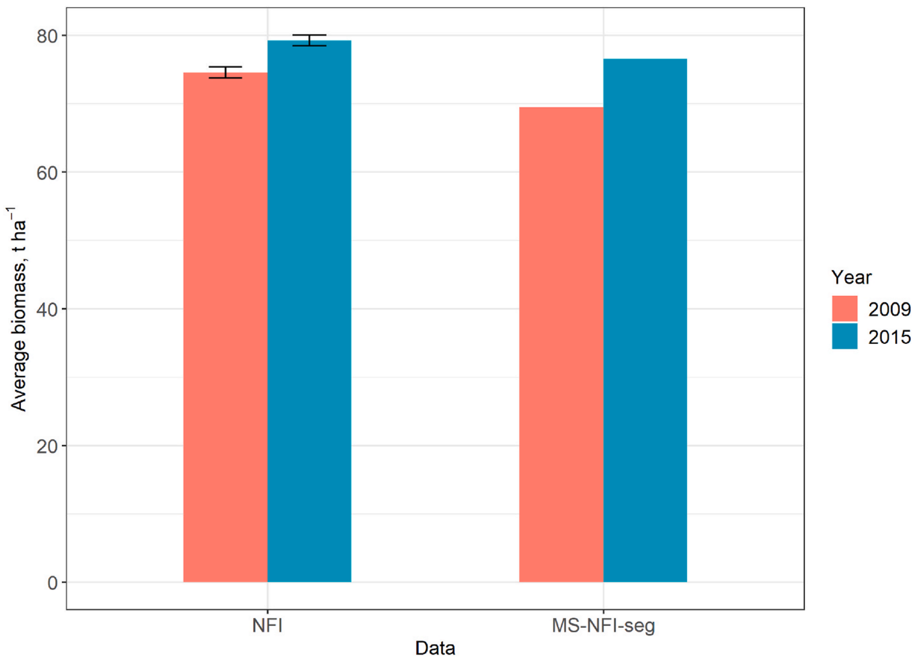

Fig. 5. Changes in living biomass between 2009 and 2015 based on NFI field plots and MS–NFI–seg data, error bars are twice the standard error.

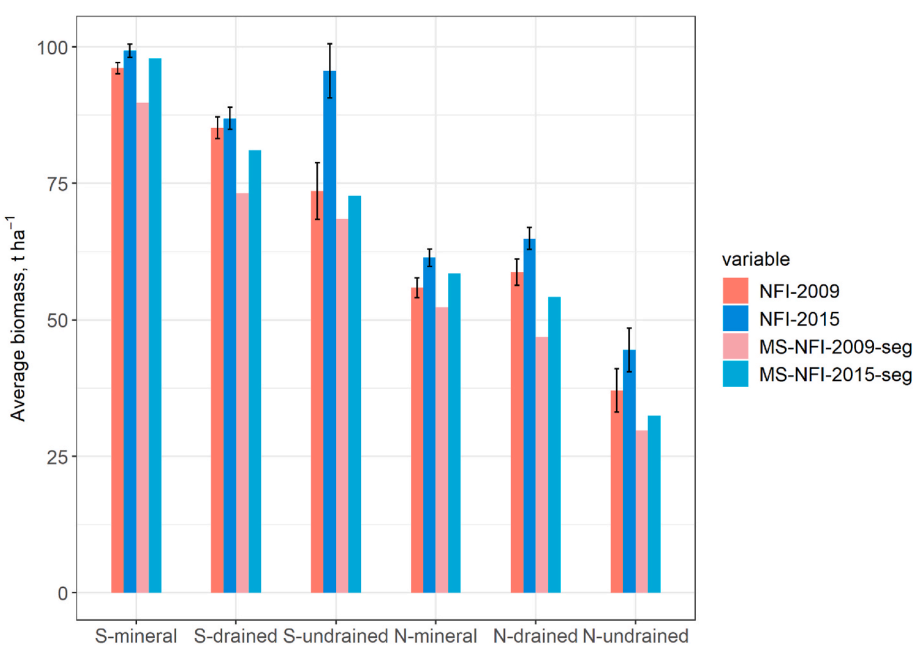

Fig. 6. Biomass in 2009 and 2015 for different soil types in southern (S) and northern (N) Finland, error bars are twice the standard error.

The biomass predictions of the MS-NFI could be improved significantly by integrating 3D remote sensing data source, e.g. in the form of ALS of stereophotogrammetric point cloud data (Baltsavias et al., 2008; St-Onge et al., 2008; Tuominen et al., 2017). The 3D point cloud data allows accurate modelling of forest canopy, thus enhancing biomass predictions, but often due to cost and availability reasons, they may be difficult to integrate with optical satellite data for large areas. In Finland, the national laser scanning rotation is currently 6 years for entire country, whereas digital aerial photography is acquired with 3 years interval, thus making it theoretically feasible for MS-NFI in relation to temporal and area coverage requirements. However, currently there is no operational procedure set up for producing such stereo-photogrammetric point cloud for the country. In subsequent MS-NFI inventories after 2015, Sentinel-2 imagery have been utilized as the main remote sensing data source, since Sentinel-2 has very good spatial, temporal and spectral resolution (Mäkisara et al., 2022).

Forest areas managed for wood production have heterogeneous age structures between stands and biomass changes are caused by relatively high growth levels or a strong decrease in biomass due to timber harvesting. Image segmentation decreases slightly for RMSEs compared to pixel-level variation. However, due to the relatively short study period, RMSE at the segment level can still exceed biomass growth and results in an unreal decrease in biomass at the segment level. Only in case of major disturbances such as clear-cuttings, when comparing MS–NFI–seg data to the GFC-seg map (Hansen et al., 2013), relative congruent areas were detected having biomass loss (Fig. 7). It would be also possible to

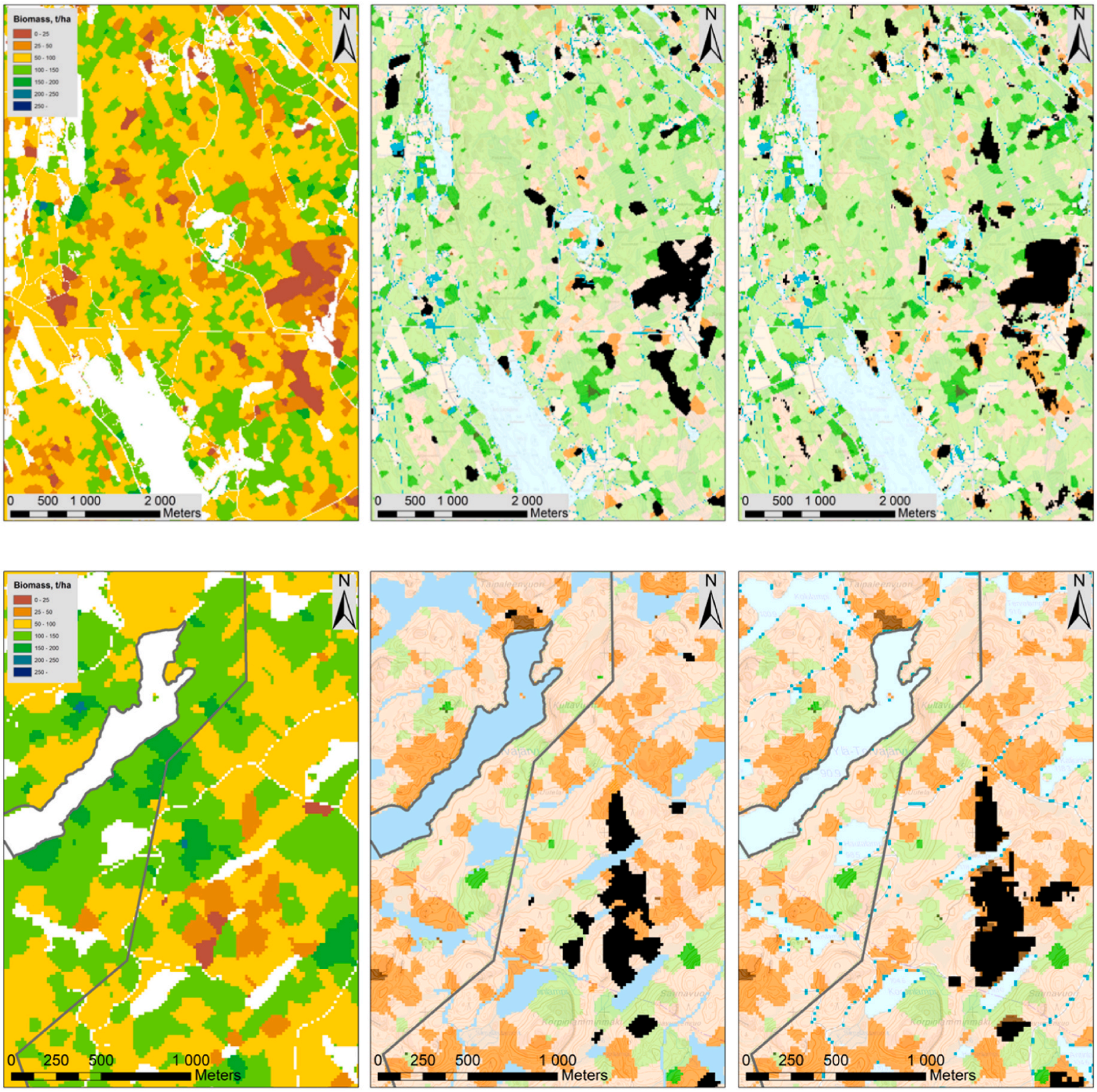

Fig. 7. Tree biomass in MS–NFI–seg data in 2015 (left), a MS–NFI–seg change map and disturbed areas on black colour (centre) and corresponding GFC-seg map (right) on forest cover loss between 2009 and 2015. Above are typical commercial forests (located in Alavus SW Finland), and below are protected and commercial forests with higher biomass (Repovesi National Park, south Finland). In the change map, the green colour indicates the amounts of gains, and the orange-brown colour shows losses. Base map is from the National Land Survey of Finland. (For interpretation of the references to colour in this figure legend, the reader is referred to the Web version of this article.)

Table 3
Confusion matrix of forest disturbance on MS–NFI–seg and GFC-seg data.

	GFC-seg			
MS–NFI–seg	Disturbed	Undisturbed	Total	Producer's Accuracy
Disturbed	554307	834476	1388783	**0.40**
Undisturbed	432041	23553325	23985366	**0.98**
Total	986348	24387801	25374149	
User's accuracy	**0.56**	**0.97**		
			Correct	**0.95**
			Kappa	**0.44**

Table 4
Comparison of disturbed areas derived from NFI plots, GFC-seg data and MS–NFI–seg data.

	NFI	GFC-seg		MS–NFI–seg	
		Disturbed	Undisturbed	Disturbed	Undisturbed
Disturbed	286	196	90	178	108
Undisturbed	7670	264	7406	189	7481
N	7956	460	7496	367	7589
Disturbed, %	3.6	2.5	1.1	2.2	1.4
Undisturbed, %	96.4	3.3	93.1	2.4	94.0
Total, %	100.0	5.8	94.2	4.6	95.4

combine the GFC-seg map to MS–NFI–seg biomass estimates to get small area estimates on total biomass lost. Harvest area estimates reported by Ceccherini et al. (2020, Extended Data Fig. 6) based also on GFC time-series and the reported average area for Finland were approximately 150,000 ha a^{-1} in the study period. However, as derived from Breidenbach et al. (2021), approximately only 100,000 ha a^{-1} was due to final harvests. The reported areas by Ceccherini et al. (2020) were quite stable during the study period but were increased between 2016 and 2018. Other studies suggest that this increase in the harvest area is merely an artifact (Breidenbach et al., 2021; Picard et al., 2021).

In recognition of disturbed areas, it would be better to focus on growing stock variables when segments are comprised. However, in terms of greenhouse gas emissions, soil type and management are key factors at the stand level to determine where potential sinks and sources are located. With this spatially explicit data, it is possible to provide input data for soil modellers to further study, on which forest management operations are appropriate for a certain type of stands to mitigate greenhouse emissions cost-effectively. Further, MS–NFI–seg data includes amount of biomass both before and after potential disturbance. This information can be applied to real forest management units, compartments, where similar information on soil and stand properties is available. The most reliable change estimates on biomass for segments were achieved on clear-cut sites. In case of smaller changes in biomass or tree volumes, time series analyses would improve the reliability of the change estimates (Katila et al., 2020).

For time series various types free and open access remote sensing data are available, e.g., Landsat satellite archive and Sentinel-2 data more recently. Wide range of satellite data products have enabled rapid development of methodologies and approaches to monitor large area forest characteristics and change. Time series analyses can be used to provide more accurate estimates of forest stands than just single-year images. Time series allow historical and current estimates of forest conditions (Bolton et al., 2020). There has been significant methodological development using satellite image time series in land cover and forest attributes estimation (Gómez et al., 2016; Hermosilla et al., 2018; Wulder et al., 2018; Bolton et al., 2020). Use of satellite data allows very large area mapping of forest biomass and other attributes. Despite the benefits related to low cost, wide area coverage and good temporal resolution of current satellite imagery, such as Sentinel-2, their low prediction accuracy at stand level remain drawback (Mäkisara et al., 2019, 2022). The 3-dimensional ALS data is considered the most accurate remote sensing data in forest biomass estimation but as costly is often limited with the coverage area and temporal resolution. Advantage of active radar based satellite sensors have capability to penetrate clouds, but otherwise they do not provide more accurate data compared to optical satellite images (Holopainen et al., 2014; Lohberger et al., 2011). GEDI satellite system provides large area 3-dimensional data but has relatively low spatial resolution.

6. Conclusions

This study presents segmented maps for tree biomass and its changes by soil type (here upland soil, peatland soil and drained peatland soil) based on MS-NFI forest attribute maps. Spatially accurate map data of biomass changes on forest land are required for optimal management alternatives in terms of climate change mitigation. At regional level and whole country level the estimated biomass stock values of MS–NFI–seg data were consistent with NFI field data. On the other hand, at forest stand level there were clear differences between the MS-MFI-seg maps and GFC-seg data on disturbed areas. In general, in detecting disturbed areas such as timber harvests, only stand-replacement changes were relatively reliably detected.

Utilizing soil type in segmenting MS-NFI maps allowed us to create management units which are more homogeneous by their climate impacts as GHG emissions vary largely between mineral soils, drained and undrained peatland soils and, in particular drained fertile peatland soils are known to be emissions hot spots. The segment-level forest maps facilitate comparison of top-down ecosystem modelling of GHG exchange by land-surface models against high resolution bottom-up that is presented here as a map. In practical forestry, decisions are made at management unit (i.e. stand) level, and for taking into account GHG exchange impact of management operations, such maps as presented here are needed for emissions estimation and decision making. In the future, the uncertainty of biomass change maps could be improved by introducing time series analysis of biomass maps of several time points. Also, the delineation of forest management units can be improved by introducing higher resolution canopy height data based on airborne laser scanning.

Funding

The study was funded by the Strategic Research Council at the Academy of Finland, Decision no. 312912 (SOMPA) and Horizon Europe (ForestPaths, project no 101056755).

Declaration of competing interest

The authors declare that they have no known competing financial interests or personal relationships that could have appeared to influence the work reported in this paper.

Acknowledgements

The authors want to thank the staff at the Natural Resources Institute Finland (Luke) for their contribution in the NFI data collection and preparation, and producing the MS-NFI thematic maps used in this study, and we also thank the greenhouse gas inventory project for their data.

Appendix A. Supplementary data

Supplementary data to this article can be found online at https://doi.org/10.1016/j.ophoto.2023.100036.

References

Avitabile, V., Camia, A., 2018. An assessment of forest biomass maps in Europe using harmonized national statistics and inventory plots. For. Ecol. Manag. 409, 489–498. https://doi.org/10.1016/j.foreco.2017.11.047.

Baltsavias, E., Gruen, A., Eisenbeiss, H., Zhang, L., Waser, L.T., 2008. High-quality image matching and automated generation of 3D tree models. Int. J. Rem. Sens. 29 (5), 1243–1259. https://doi.org/10.1080/01431160701736513.

Barrett, F., McRoberts, R.E., Tomppo, E., Cienciala, E., Waser, L.T., 2016. A questionnaire-based review of the operational use of remotely sensed data by national forest inventories. Remote Sens. Environ. 2016 (174), 279–289. https://doi.org/10.1016/j.rse.2015.08.029.

Bolton, D.K., Tompalski, P., Coops, N.C., White, J.C., Wulder, M.A., Hermosilla, T., et al., 2020. Optimizing Landsat time series length for regional mapping of lidar-derived forest structure. Rem. Sens. Environ. 239, 111645 https://doi.org/10.1016/j.rse.2020.111645.

Breidenbach, J., Ellison, D., Petersson, H., Korhonen, K., Henttonen, H., Wallerman, J., et al., 2021. No" Abrupt increase in harvested forest area over Europe after 2015"-How the misuse of a satellite-based map led to completely wrong conclusions. In: EGU General Assembly Conference Abstracts. EGU21-13243). https://ui.adsabs.harvard.edu/link_gateway/2021EGUGA..2313243B/doi:10.5194/egusphere-egu21-13243.

Ceccherini, G., Duveiller, G., Grassi, G., Lemoine, G., Avitabile, V., Pilli, R., Cescatti, A., 2020. Abrupt increase in harvested forest area over Europe after 2015. Nature 583 (7814), 72–77. https://doi.org/10.1038/s41586-020-2438-y.

Egusa, T., Kumagai, T.O., Shiraishi, N., 2020. Carbon stock in Japanese forests has been greatly underestimated. Sci. Rep. 10 (1), 1–9. https://doi.org/10.1038/s41598-020-64851-2.

European Environment Agency, 2021. Annual European Union greenhouse gas inventory 1990–2019 and inventory report 2021. Submission to the UNFCCC Secretariat 27 (May 2021). EEA/PUBL/2021/066. https://www.eea.europa.eu/publications/annual-european-union-greenhouse-gas-inventory-2021. (Accessed 14 February 2021).

Franco-Lopez, H., Ek, A.R., Bauer, M.E., 2001. Estimation and mapping of forest stand density, volume, and cover type using the k-nearest neighbors method. Remote Sens. Environ. 77 (3), 251–274. https://doi.org/10.1016/S0034-4257(01)00209-7.

Franke, A.K., Feilhauer, H., Bräuning, A., Rautio, P., Braun, M., 2019. Remotely sensed estimation of vegetation shifts in the polar and alpine tree-line ecotone in Finnish Lapland during the last three decades. For. Ecol. Manag. 454, 117668 https://doi.org/10.1016/j.foreco.2019.117668.

Fu, K.S., Mui, J.K., 1981. A survey of image segmentation. Pattern Recogn. 13 (1), 3–16.

Gallaun, H., Zanchi, G., Nabuurs, G.J., Hengeveld, G., Schardt, M., Verkerk, P.J., 2010. EU-wide maps of growing stock and above-ground biomass in forests based on remote sensing and field measurements. For. Ecol. Manag. 260 (3), 252–261.

Gjertsen, A.K., 2007. Accuracy of forest mapping based on Landsat TM data and a kNN-based method. Remote Sens. Environ. 110, 420–430. https://doi.org/10.1016/j.rse.2006.08.018.
Gómez, C., White, J.C., Wulder, M.A., 2016. Optical remotely sensed time series data for land cover classification: a review. ISPRS J. Photogrammetry Remote Sens. 116, 55–72. https://doi.org/10.1016/j.isprsjprs.2016.03.008.
Hall, R.J., Skakun, R.S., Arsenault, E.J., Case, B.S., 2006. Modeling forest stand structure attributes using Landsat ETM+ data: application to mapping of aboveground biomass and stand volume. For. Ecol. Manag. 225 (1-3), 378–390. https://doi.org/10.1016/j.foreco.2006.01.014.
Hansen, M.C., Defries, R.S., Townshend, J.R.G., Carroll, M., Dimiceli, C., Sohlberg, R.A., 2003. Global percent tree cover at a spatial resolution of 500 meters: first results of the modis vegetation continuous fields algorithm. Earth Interact. 7, 1–15. https://doi.org/10.1175/1087-3562(2003)007<0001:GPTCAA>2.0.CO;2.
Hansen, M.C., Potapov, P.V., Moore, R., Hancher, M., Turubanova, S.A., Tyukavina, A., et al., 2013. High-resolution global maps of 21st-century forest cover change. Science 342 (6160), 850–853. https://doi.org/10.1126/science.1244693.
Haralick, R.M., Shapiro, L.G., 1985. Survey: image segmentation techniques. Comput. Vis. Graph Image Process 29 (1), 100–132.
Hermosilla, T., Wulder, M.A., White, J.C., Coops, N.C., Hobart, G.W., 2018. Disturbance-informed annual land cover classification maps of Canada's forested ecosystems for a 29-year Landsat time series. Can. J. Rem. Sens. 44 (2018), 1–21. https://doi.org/10.1080/07038992.2018.1437719.
Herold, M., Carter, S., Avitabile, V., Espejo, A.B., Jonckheere, I., Lucas, R., et al., 2019. The role and need for space-based forest biomass-related measurements in environmental management and policy. Surv. Geophys. 40 (4), 757–778. https://doi.org/10.1007/s10712-019-09510-6.
Hirata, Y., Tabuchi, R., Patanaponpaiboon, P., Poungparn, S., Yoneda, R., Fujioka, Y., 2014. Estimation of aboveground biomass in mangrove forests using high-resolution satellite data. J. For. Res. 19 https://doi.org/10.1007/s10310-013-0402-5.
Holopainen, M., Vastaranta, M., Hyyppä, J., 2014. Outlook for the next generation's precision forestry in Finland. Forests 5 (7), 1682–1694. https://doi.org/10.3390/f5071682.
Häkkilä, M., Le Tortorec, E., Brotons, L., Rajasärkkä, A., Tornberg, R., Mönkkönen, M., 2017. Degradation in landscape matrix has diverse impacts on diversity in protected areas. PLoS One 12 (9), e0184792. https://doi.org/10.1371/journal.pone.0184792.
ISPRA, 2021. Moving to the 2006 IPCC Guidelines for UNFCCC Reporting, vol. 2021. ISPRA Rapporti, p. 358, 2021.
Katila, M., Heikkinen, J., 2020. Reducing error in small-area estimates of multi-source forest inventory by multi-temporal data fusion. Forestry: Int. J. Financ. Res. 93 (3), 471–480. https://doi.org/10.1093/foresj/cpz076.
Katila, M., Rajala, T., Kangas, A., 2020. Assessing local trends in indicators of ecosystem services with a time series of forest resource maps. Silva Fenn. 54 (4), 10347 https://doi.org/10.14214/sf.10347, 19.
Katila, M., Tomppo, E., 2001. Selecting estimation parameters for the Finnish multisource national forest inventory. Rem. Sens. Environ. 76 (1), 16–32. https://doi.org/10.1016/S0034-4257(00)00188-7.
Kim, S.R., Lee, W.K., Kwak, D.A., Biging, G.S., Gong, P., Lee, J.H., Cho, H.K., 2011. Forest cover classification by optimal segmentation of high resolution satellite imagery. Sensors 11 (2), 1943–1958. https://doi.org/10.3390/s110201943.
Kindermann, G., McCallum, I., Fritz, S., Obersteiner, M., 2008. A global forest growing stock, biomass and carbon map based on FAO statistics. Silva Fenn. 42 (3), 387–396. https://doi.org/10.14214/sf.244.
Korhonen, K.T., Ahola, A., Heikkinen, J., Henttonen, H.M., Hotanen, J.-P., Ihalainen, A., Melin, M., Pitkänen, J., Räty, M., Sirviö, M., Strandström, M., 2021. Forests of Finland 2014–2018 and their development 1921–2018. Silva Fenn. 55 (5), 10662 https://doi.org/10.14214/sf.10662, 49.
Korhonen, K.T., Ihalainen, A., Ahola, A., Heikkinen, J., Henttonen, H.M., Hotanen, J.-P., Nevalainen, S., Pitkänen, J., Strandström, M., Viiri, H., 2017. Suomen metsät 2009–2013 ja niiden kehitys 1921–2013. Luonnonvara- ja biotalouden tutkimus 59/2017. Luonnonvarakeskus, Helsinki, p. 86.
Korhonen, K.T., Ihalainen, A., Viiri, H., Heikkinen, J., Henttonen, H.M., Hotanen, J.-P., Mäkelä, H., Nevalainen, S., Pitkänen, J., 2013. Suomen metsät 2004–2008 ja niiden kehitys 1921–2008. Metsätieteen aikakauskirja 3, 269–608. https://doi.org/10.14214/ma.6025.
Leifeld, J., Menichetti, L., 2018. The underappreciated potential of peatlands in global climate change mitigation strategies. Nat. Commun. 9 (1), 1071. https://doi.org/10.1038/s41467-018-03406-6.
Li, Y., Li, M., Li, C., et al., 2020. Forest aboveground biomass estimation using Landsat 8 and Sentinel-1A data with machine learning algorithms. Sci. Rep. 10, 9952. https://doi.org/10.1038/s41598-020-67024-3.
Lohberger, S., Keuck, V., Siegert, F., 2011. Tropical forest biomass assessment using multi-frequency radar imagery. SPIE Newsroom. https://doi.org/10.1117/2.1201108.003684.
Luonnonvarakeskus, 2019. Statistics database. Forest statistics. https://statdb.luke.fi/PXWeb/pxweb/en/LUKE/. (Accessed 29 April 2019).
Luonnonvarakeskus, 2022. Statistics database. Forest statistics. https://statdb.luke.fi/PXWeb/pxweb/en/LUKE/. (Accessed 14 February 2022).
McRoberts, R.E., Nelson, M.D., Wendt, D.G., 2002. Stratified estimation of forest area using satellite imagery, inventory data, and the k-Nearest Neighbors technique. Rem. Sens. Environ. 82 (2-3), 457–468. https://doi.org/10.1016/S0034-4257(02)00064-0.
Mustonen, J., Packalén, P., Kangas, A., 2008. Automatic segmentation of forest stands using a canopy height model and aerial photography. Scand. J. For. Res. 23 (6), 534–545. https://doi.org/10.1080/02827580802552446.
Mäkisara, K., Katila, M., Peräsaari, J., Tomppo, E., 2016. The Multi-Source National Forest Inventory of Finland – Methods and Results 2013. Natural Resources Institute Finland (Luke). https://jukuri.luke.fi/handle/10024/532147 (Luke).
Mäkisara, K., Katila, M., Peräsaari, J., 2019. The multi-source national forest inventory of Finland –methods and results 2015. In: Natural Resources and Bioeconomy Studies, vol. 8. Natural Resources Institute Finland, Helsinki, p. 57, 2019. http://urn.fi/URN:ISBN:978-952-326-711-4. (Accessed 26 April 2019).
Mäkisara, K., Katila, M., Peräsaari, J., 2022. The Multi-Source national forest Inventory of Finland — methods and Results 2017 and 2019. Natural Resources and bioeconomy Studies, vol. 90. Natural Resources Institute Finland, Helsinki, p. 73, 2022.
Narendra, P.M., Goldberg, M., 1980. Image segmentation with directed trees. IEEE 762 transactions on pattern analysis and machine intelligence PAMI-2, 185–191.
Nilsson, M., Nordkvist, K., Jonzén, J., Lindgren, N., Axensten, P., Wallerman, J., et al., 2017. A nationwide forest attribute map of Sweden predicted using airborne laser scanning data and field data from the National Forest Inventory. Remote Sens. Environ. 194, 447–454. https://doi.org/10.1016/j.rse.2016.10.022.
Pekkarinen, A., 2002. Image segment-based spectral features in the estimation of timber volume. 787. Rem. Sens. Environ. 82, 349–359.
Pekkarinen, A., 2004. Image Segmentation in multi-Source forest Inventory. Finnish Forest Research Institute, Vantaa Research Centre.
Picard, N., Leban, J.M., Guehl, J.M., Dreyer, E., Bouriaud, O., Bontemps, J.D., et al., 2021. Recent increase in European forest harvests as based on area estimates (Ceccherini et al. 2020a) not confirmed in the French case. Ann. For. Sci. 78 (1), 1–5. https://doi.org/10.1007/s13595-021-01030-x.
Pukkala, T., 2020. Delineating forest stands from grid data. For. Ecosyst. 2020, 7–13. https://doi.org/10.1186/s40663-020-00221-8.
Reese, H., Nilsson, M., Pahlén, T.G., Hagner, O., Joyce, S., Tingelöf, U., et al., 2003. Countrywide estimates of forest variables using satellite data and field data from the National Forest Inventory. Ambio 32, 542–548.
Repola, J., 2008. Biomass equations for birch in Finland. Silva Fenn. 42 (4), 605–624.
Repola, J., 2009. Biomass equations for Scots pine and Norway spruce in Finland. Silva Fenn. 43 (4), 625–647.
Repola, J., Ojansuu, R., Kukkola, M., 2007. Biomass functions for Scots pine, Norway spruce and birch in Finland. Metla Working Paper 2007 (53), 28.
Rodríguez-Veiga, P., Saatchi, S., Tansey, K., Balzter, H., 2016. Magnitude, spatial distribution and uncertainty of forest biomass stocks in Mexico. Rem. Sens. Environ. 183, 265–281. https://doi.org/10.1016/j.rse.2016.06.004.
Saarela, S., Holm, S., Healey, S.P., Andersen, H.-E., Petersson, H., Prentius, W., Patterson, P.L., Næsset, E., Gregoire, T.G., Ståhl, G., 2018. Generalized Hierarchical model-based estimation for aboveground biomass assessment using GEDI and Landsat data. Rem. Sens. 10 (11), 1832. https://doi.org/10.3390/rs10111832.
Saarela, S., Wästlund, A., Holmström, E., et al., 2020. Mapping aboveground biomass and its prediction uncertainty using LiDAR and field data, accounting for tree-level allometric and LiDAR model errors. For. Ecosyst. 2020, 7–43. https://doi.org/10.1186/s40663-020-00245-0.
Statistics Finland, 2021. Greenhouse Gas Emissions in Finland 1990 to 2019. In: National Inventory Report under the UNFCCC and the Kyoto Protocol. (Accessed 15 April 2021).
St-Onge, B., Vega, C., Fournier, R.A., Hu, Y., 2008. Mapping canopy height using a combination of digital stereo-photogrammetry and lidar. Int. J. Rem. Sens. 29 (11), 3343–3364. https://doi.org/10.1080/01431160701469040.
Tokola, T., LeToan, T., Poncet, v., F, Tuominen, S., Holopainen, M., 2007. Forest reconnaissance surveys: comparison of estimates based on simulated TerraSAR, and optical data. Photogramm. J. Finland 20 (2), 64–79.
Tomppo, E., 1991. Satellite image-based national forest inventory of Finland. Int. Archives Photogrammetry Remote Sens. 1991 (28), 419–424.
Tomppo, E., 2006. The Finnish multi-source national forest inventory - small area estimation and map production. In: Kangas, A., Maltamo, M. (Eds.), Forest Inventory. Methodology and Applications, Managing Forest Ecosystems, vol. 10. Springer, Dordrecht, The Netherlands, pp. 195–224.
Tomppo, E., Halme, M., 2004. Using coarse scale forest variables as ancillary information and weighting of variables in k-nn estimation: a genetic algorithm approach. Rem. Sens. Environ. 92, 1–20. https://doi.org/10.1016/j.rse.2004.04.003.
Tomppo, E., Haakana, M., Katila, M., Peräsaari, J., 2008a. Multi-source national forest inventory - Methods and applications. In: Series: Managing Forest Ecosystems, Vol. 18. Springer. https://doi.org/10.1007/978-1-4020-8713-4. XIV. 374 p.
Tomppo, E., Heikkinen, J., Henttonen, H.M., Ihalainen, A., Katila, M., Mäkelä, H., Tuomainen, T., Vainikainen, N., 2011. Designing and Conducting a forest Inventory-Case: 9th National Forest Inventory of Finland, vol. 22. Springer.
Tomppo, E., Katila, M., Mäkisara, K., Peräsaari, J., 2013. The multi-source national forest inventory of Finland –methods and results 2009. Working Papers of the Finnish Forest Research Institute 273, 216. http://www.metla.fi/julkaisut/workingpapers/2013/mwp273.pdf. (Accessed 26 April 2019).
Tomppo, E., Olsson, H., Ståhl, G., Nilsson, M., Hagner, O., Katila, M., 2008b. Combining national forest inventory field plots and remote sensing data for forest databases. Rem. Sens. Environ. 112 (Issue 5), 1982–1999. Elsevier. https://doi.org/10.1016/j.rse.2007.03.032. (Accessed 15 May 2008).
Tuominen, S., Eerikäinen, K., Schibalski, A., Haakana, M., Lehtonen, A., 2010. Mapping biomass variables with a multi-source forest inventory technique. Silva Fenn. 44 (1), 458 https://doi.org/10.14214/sf.458.
Tuominen, S., Haapanen, R., 2013. Estimation of forest biomass by means of genetic algorithm-based optimization of airborne laser scanning and digital aerial photograph features. Silva Fenn. 47 (1), 902 https://doi.org/10.14214/sf.902.

Tuominen, S., Pitkänen, T.P., Balazs, A., Kangas, A., 2017. Improving Finnish multi-source national forest inventory by 3D aerial imaging. Silva Fenn. 51 (4), 7743 https://doi.org/10.14214/sf.7743.

Vastaranta, M., Niemi, M., Karjalainen, M., Peuhkurinen, J., Kankare, V., Hyyppä, J., Holopainen, M., 2014. Prediction of forest stand attributes using TerraSAR-X stereo imagery. Rem. Sens. 6 (4), 3227–3246. https://doi.org/10.3390/rs6043227.

Vangi, E., D'Amico, G., Francini, S., Borghi, C., Giannetti, F., Corona, P., et al., 2023. Large-scale high-resolution yearly modeling of forest growing stock volume and above-ground carbon pool. Environ. Model. Software 159, 105580. https://doi.org/10.1016/j.envsoft.2022.105580.

Wulder, M.A., Coops, N.C., Roy, D.P., White, J.C., Hermosilla, T., 2018. Land cover 2.0. Int. J. Rem. Sens. 39 (2018), 4254–4284. https://doi.org/10.1080/01431161.2018.1452075.

Yu, Q., Gong, P., Clinton, N., Biging, G., Kelly, M., Schirokauer, D., 2006. Object-based detailed vegetation classification with airborne high spatial resolution remote sensing imagery. Photogramm. Eng. Rem. Sens. 72 (7), 799–811. https://doi.org/10.14358/PERS.72.7.799.

Zhao, P., Lu, D., Wang, G., Wu, C., Huang, Y., Yu, S., 2016. Examining spectral reflectance saturation in Landsat imagery and corresponding solutions to improve forest aboveground biomass estimation. Rem. Sens. 8 (6), 469. https://doi.org/10.3390/rs8060469.

Zheng, D., Rademacher, J., Chen, J., Crow, T., Bresee, M., Le Moine, J., Ryu, S.R., 2004. Estimating aboveground biomass using Landsat 7 ETM+ data across a managed landscape in northern Wisconsin, USA. Remote Sens. Environ. 93 (3), 402–411. https://doi.org/10.1016/j.rse.2004.08.008.